5. Fractals in Theoretical Physics

This final chapter is intended to be read as a 'dessert' – a kind of reward for having worked through the four main pillars of theoretical physics presented thus far. No background from the previous chapters is assumed, so the reader who skips the main meal is nonetheless welcome to taste the dessert. We won't be like the conscientious wife who denied her dying husband's last wish – to taste the freshly baked cakes whose odor drifted from her kitchen to his deathbed – with the scolding remark "The cakes are for *after* the funeral!"

Plato sought to explain nature with five regular solids; Newton and Kepler bent Plato's circle to an ellipse; modern science analyzed Plato's shapes into particles and waves, and generalized the curves of Newton and Kepler to relative probabilities – still without a single 'rough edge.' Now, more than two thousand years after Plato, nearly three hundred years after Newton, and after thirty strenuous years of wily insinuation, calculated argument, and stunning demonstration, Benoit Mandelbrot has established a discovery that ranks with the laws of *regular* motion. Bespeaking the knowledge possessed by every child and every great painter, Mandelbrot has observed, "Clouds are not spheres, mountains are not cones, coastlines are not circles, bark is not smooth, nor does lightning travel in a straight line."

What Mandelbrot has named fractal geometry describes not only the zigzag of Zeus's thunderbolt, or the branching and the varying densities of Pan's forests. It describes as well the Mercurial irregularities of the commodities market, the heretofore unaccountable fits of Poseidon the earthshaker, and a myriad of phenomena in the realm of lesser deities – snowflakes, shale, lava, gels, the rise and fall of rivers, fibrillations of the heart, the surging of electronic noise. Fractal geometry points to a symmetry of pattern within each of the meldings, branchings, and shatterings of nature.

A book that preceded by more than half a century Mandelbrot's 1982 classic *The Fractal Geometry of Nature* and was known by every scientist at that time is *On Growth & Form* by W. D'Arcy Thompson (1917). *On Growth & Form* called attention to the fact that a large part of science was based on structures and processes that on a microscopic level are completely random, despite the fact that on the macroscopic level we can perceive *patterns* and *structure*. This classic has become popular again, in large part due to the fact that in the past few years the advent of advanced computing and sophisticated experimental techniques have led to dramatic progress in our understanding of the connection between the structure of a variety of random 'forms' and the fashion in which these

forms 'grow.' Not surprisingly, within the scientific community there has been a tremendous upsurge of interest in this opportunity to unify a large number of diverse phenomena, ranging from chemistry and biology to physics and materials science.

5.1 Non-random Fractals

Fractals fall into two categories, *random* (Plate 1) and *non-random* (Plate 2). Fractals in physics belong to the first category, but it is instructive to discuss first a much-studied example of a non-random fractal – the Sierpinski gasket. We simply iterate a *growth rule* much as a child might assemble a castle from building blocks. Our basic unit is a triangular-shaped tile shown in Fig. 5.1a, which we take to be of unit 'mass' ($M = 1$) and of unit edge length ($L = 1$).

The Sierpinski gasket is defined operationally as an 'aggregation process' obtained by a simple iterative process. In stage one, we join three tiles together to create the structure shown in Fig. 5.1b, an object of mass $M = 3$ and edge $L = 2$. The effect of stage one is to produce a unit with a lower density: if we define the density as

$$\varrho(L) \equiv M(L)/L^2, \tag{5.1}$$

then the density decreases from unity to 3/4 as a result of stage one.

Now simply iterate – i.e., repeat this growth rule over and over *ad infinitum*. Thus in stage two, join together – as in Fig. 5.1c – three of the $\varrho = 3/4$ structures constructed in stage one, thereby building an object with $\varrho = (3/4)^2$. In stage three, join three objects identical to those constructed in stage two. Continue until you run out of tiles (if you are a physicist) or until the structure is infinite (if

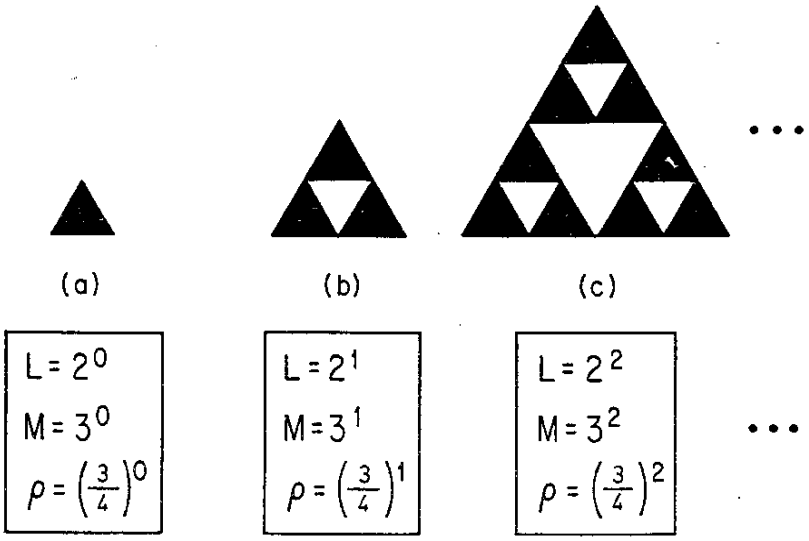

Fig. 5.1a–c. First few stages in the aggregation rule which is iterated to form a Sierpinski gasket fractal.

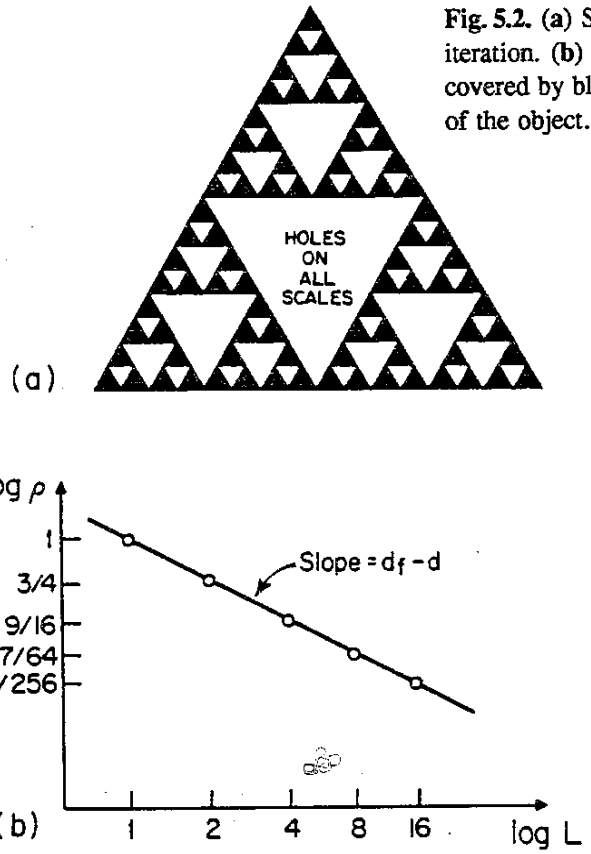

Fig. 5.2. (a) Sierpinski gasket fractal after four stages of iteration. (b) A log-log plot of ϱ, the fraction of space covered by black tiles, as a function of L, the linear size of the object.

you are a mathematician!). The result after stage four – with 81 black tiles and 175 white tiles (Fig. 5.2a) may be seen to this day in floor mosaics of the church in Anagni, Italy, which was built in the year 1104 (Plate 2). Thus although the Sierpinski gasket fractal is named after a 20th century Polish mathematician, it was known some eight centuries earlier to every churchgoer of this village!

The citizens of Anagni did not have double-logarithmic graph paper in the 12th century. If they had had such a marvelous invention, then they might have plotted the dependence of ϱ on L. They would find Fig. 5.2b, which displays two striking features:

- $\varrho(L)$ decreases monotonically with L, without limit, so that by iterating sufficiently we can achieve an object of *as low a density as we wish*, and
- $\varrho(L)$ decreases with L in a *predictable* fashion, namely a simple power law.

Power laws have the generic form $y = \mathcal{A}x^{\alpha}$ and, as such, have two parameters, the 'amplitude' $\mathcal{A}$ and the exponent α. The amplitude is not of intrinsic interest, since it depends on the choice we make for the definitions of M and L. The exponent, on the other hand, depends on the process itself – i.e., on the 'rule' that we follow when we iterate. In short, different rules give different exponents. In the present example, $\varrho(L) = L^{\alpha}$ so the amplitude is unity. The exponent is given by the slope of Fig. 5.2b,

$$\alpha = \text{slope} = \frac{\log 1 - \log(3/4)}{\log 1 - \log 2} = \frac{\log 3}{\log 2} - 2. \tag{5.2}$$

Finally we are ready to define the fractal dimension d_f, through the equation

$$M(L) \equiv \mathcal{A}\, L^{d_f}. \tag{5.3}$$

If we substitute (5.3) into (5.1), we find

$$\varrho(L) = \mathcal{A}\, L^{d_f - 2}. \tag{5.4}$$

Comparing (5.2) and (5.4), we conclude that the Sierpinski gasket is indeed a fractal object with fractal dimension

$$d_f = \log 3 / \log 2 = 1.58\ldots \tag{5.5}$$

Classical (Euclidean) geometry deals with regular forms having a dimension the same as that of the embedding space. For example, a line has $d = 1$, and a square $d = 2$. We say that the Sierpinski gasket has a dimension intermediate between that of a line and a square.

We may generalize the Sierpinski gasket from $d = 2$ to $d = 3$, taking as the basic building block a regular tetrahedron of edge $L = 1$ and mass $M = 1$. Combining *four* such blocks we can build a $L = 2$ tetrahedron with a hole in the center – so that $M = 4$ for $L = 2$, and this construction may be iterated indefinitely to form an object resembling the Great Pyramid after a termite attack. We see that $d_f = 2$, so for this example the fractal dimension is an integer! We offer as an amusing exercise to generalize the Sierpinski gasket structure to an embedding space of *arbitrary* dimension d (yes, we can have exercises during dessert, provided that they are amusing). You should find the result

$$d_f = \log(d+1) / \log 2. \tag{5.6}$$

5.2 Random Fractals: The Unbiased Random Walk

Real systems in nature do not resemble the floor of the Anagni church – in fact, no non-random fractals are found in Nature. What is found are objects which themselves are not fractals but which have the remarkable feature that if we form a *statistical average* of some property such as the density, we find a quantity that decreases linearly with length scale when plotted on double logarithmic paper. Such objects are termed *random fractals*, to distinguish them from the non-random *geometric fractals* discussed in the previous section.

Consider the following prototypical problem in statistical mechanics. At time $t = 0$ an ant[1] is parachuted to an arbitrary vertex of an infinite one-dimensional

[1] The use of the term *ant* to describe a random walker is used almost universally in the theoretical physics literature – perhaps the earliest reference to this colorful animal is a 1976 paper of de Gennes that succeeded in formulating several general physics problems in terms of the motion of a 'drunken' ant with appropriate rules for motion. Generally speaking, *classical* mechanics concerns itself with the prediction of the position of a 'sober' ant, given some set of non-random forces acting on it, while *statistical* mechanics is concerned with the problem of predicting the position of a drunken ant.

lattice with lattice constant unity: we say $x_{t=0} = 0$. The ant carries an *unbiased* two-sided coin, and a metronome of period one. The dynamics of the ant is governed by the following rule. At each 'tick' of the metronome, it tosses the coin. If the coin is heads, the ant steps to the neighboring vertex on the East [$x_{t=1} = 1$]. If the coin is tails, it steps to the nearest vertex on the West [$x_{t=1} = -1$].

Are there *laws of nature* that govern the position of this drunken ant? At first thought, the response is likely to be *"NO – How can you predict the position of something that is random?"* However, if you have reached this far in a primer on theoretical physics, then you can imagine that there may be laws governing even the motion of random systems.

For the drunken ant described above, the first 'law' concerns $\langle x \rangle_t$, the expectation value of the position of the ant after a time t. In general, the expectation value of *any* quantity A is given by

$$\langle A \rangle \equiv \sum_c A_c P_c, \tag{5.7}$$

where A_c is the value of the quantity A in configuration c, P_c is the probability of configuration c, and the summation is over all configurations. For the example at hand, there are 2 configurations at time $t = 1$ with $P_c = 1/2$, 4 configurations at time $t = 2$ with $P_c = 1/4$. In general, there are 2^t configurations at an arbitrary time t, each with probability $P_c = (1/2)^t$. Thus

$$\langle x \rangle_t = \sum_c x_c P_c = 0. \tag{5.8}$$

for $t = 1$. To prove (5.8) in general, proceed by induction: assume (5.8) holds for time t and show that it holds for time $t + 1$.

For *non-random* systems, it is generally sufficient to predict the position of the system at time t – the analog of $\langle x \rangle_t$. For *random* systems, on the other hand, the information contained in $\langle x \rangle_t$ does not describe the system extensively. For example, we know intuitively that as time progresses, the average of the *square* of the displacement of the ant increases monotonically. The explicit form of this increase is contained in the second 'law' concerning the *mean square displacement*

$$\langle x^2 \rangle_t = t. \tag{5.9}$$

Equation (5.9) may also be proved by induction, by demonstrating that (5.9) implies $\langle x^2 \rangle_{t+1} = t + 1$.

Additional information is contained in the expectation values of higher powers of x, such as $\langle x^3 \rangle_t$, $\langle x^4 \rangle_t$, and so forth. By the same symmetry arguments leading to (5.8), we can see that $\langle x^k \rangle_t = 0$ for all *odd* integers k. However $\langle x^k \rangle_t$ is non-zero for *even* integers. Consider, e.g., $\langle x^4 \rangle_t$. We may easily verify that

$$\langle x^4 \rangle_t = 3t^2 - 2t = 3t^2 \left[1 - \frac{2/3}{t} \right]. \tag{5.10}$$

5.3 'A Single Length'

5.3.1 The Concept of a Characteristic Length

Let us compare (5.9) and (5.10). What is the displacement of the randomly walking ant? On the one hand, we might consider identifying this displacement with a length $\mathcal{L}_2$ defined by

$$\mathcal{L}_2 \equiv \sqrt{\langle x^2 \rangle} = t^{1/2}. \tag{5.11}$$

On the other hand, it is just as reasonable to identify this displacement with the length $\mathcal{L}_4$ defined by

$$\mathcal{L}_4 \equiv \sqrt[4]{\langle x^4 \rangle} = \sqrt[4]{3}\, t^{1/2} \left[1 - \frac{2/3}{t}\right]^{1/4}. \tag{5.12}$$

The important point is that both lengths display an asymptotic dependence on the time. We call the leading exponent (i.e. 1/2) the *scaling exponent*, while the non-leading exponents are termed *corrections-to-scaling*. The reader may verify that the same scaling exponent is found if we consider any length $\mathcal{L}_k$ (provided k is even),

$$\mathcal{L}_k \equiv \sqrt[k]{\langle x^k \rangle} = \mathcal{A}_k\, t^{1/2} \left[1 + \mathcal{B}_k t^{-1} + \mathcal{C}_k t^{-2} + \cdots + \mathcal{O}(t^{-k/2+1})\right]^{1/k}. \tag{5.13}$$

The subscripts on the amplitudes indicate that these depend on k. Equation (5.13) exemplifies a robust feature of random systems: *regardless of the definition of the characteristic length, the same scaling exponent describes the asymptotic behavior*. We say that all lengths scale as the square root of the time, meaning that whatever length $\mathcal{L}_k$ we choose to examine, $\mathcal{L}_k$ will *double* whenever the time has increased by a factor of *four*. This scaling property is not affected by the fact that the amplitude $\mathcal{A}_k$ in (5.13) depends on k, since we do not inquire about the absolute value of the length $\mathcal{L}_k$ but only enquire how $\mathcal{L}_k$ *changes* when t changes.

5.3.2 Higher Dimensions

Next, we shall show that the identical *scaling laws* hold for dimensions above one. Suppose we replace our one-dimensional linear chain lattice with a two-dimensional square lattice. This entails replacing our ant's coin with a four-sided bone.[2] According to the outcome of the 'bone toss', the ant will step North, East, South, or West. The coordinate of the ant is represented by a two-dimensional vector $\boldsymbol{r}(t)$ with Cartesian components $[x(t), y(t)]$.

[2] Montroll and Shlesinger have written that ancient cave men (and presumably cave women) were fascinated by games of chance and would actually roll four-sided bones to randomly choose one of four possible outcomes.

The analogs of (5.8) and (5.9) are

$$\langle \boldsymbol{r} \rangle_t = 0 \tag{5.14}$$

and

$$\langle |\boldsymbol{r}|^2 \rangle_t = t. \tag{5.15}$$

We may formally prove (5.14) and (5.15) by induction. Equation (5.15) may also be 'understood' if we note that, on average, for half the metronome ticks the ant steps either to the East or to the West, so from (5.9) the x-displacement should follow the law $\langle x^2 \rangle_t = t/2$. The other half of the time the ant moves North or South, so $\langle y^2 \rangle_t = t/2$. Hence $\langle |\boldsymbol{r}|^2 \rangle_t = \langle x^2 \rangle_t + \langle y^2 \rangle_t = t$.

For the fourth moment, we find

$$\langle |\boldsymbol{r}|^4 \rangle_t = 2t^2 \left[1 - \frac{1/2}{t} \right]. \tag{5.16}$$

Thus the length $\mathcal{L}_4$ defined in (5.12) scales with the *same* scaling exponent for two dimensions as for one dimension; the amplitudes of the leading terms and the 'correction-to-scaling' term are changed, but the asymptotic scaling properties are not affected in passing from $d = 1$ to $d = 2$. A hallmark of modern critical phenomena is that the *exponents* are quite robust but *amplitudes depend more sensitively* on what particular system is being studied.

5.3.3 Additional Lengths that Scale with $\sqrt{t}$

Linear polymers are topologically linear chains of monomers held together by chemical bonds (like a string of beads). Let us make an oversimplified model of such a linear polymer by assuming that the chain of monomers adopts a conformation in three-dimensional space that has the same statistics as the *trail* of the ant. By the trail we mean the object formed if the ant leaves behind a little piece of bread at each site visited. After a time t, the ant has left behind t pieces of bread; hence the analog of the time is the number of monomers in the polymer chain. An unrealistic feature of this simple model arises whenever the ant re-visits the same site. Then more than one piece of bread occupies the same site, while two monomers *cannot* occupy the same point of space. In Sect. 5.8, we shall see that statistical properties of a random walk provide a useful upper bound on the properties of real polymers, and that this upper bound becomes the exact value of d_f for space dimensions above a critical dimension d_c.

We can experimentally measure the radius of gyration R_g of this random walk model of a polymer. Moreover, it is a simple exercise to demonstrate that

$$R_g = \frac{1}{\sqrt{6}} R_{EE}, \tag{5.17}$$

where $R_{EE} = \sqrt{\langle |\boldsymbol{r}|^2 \rangle}$ is the Pythagorean distance between the first and last monomer; R_{EE} is called the end-to-end distance of the random walk. Thus we

expect that R_g scales as the square root of the number of monomers, just as the lengths $\mathcal{L}_2$ and $\mathcal{L}_4$ of (5.11) and (5.12) scale as the square root of the time.

Thus we find identical scaling properties no matter what definition we choose – the moment $\mathcal{L}_k$ of (5.13), the radius of gyration R_g of the trail, or the end-to-end displacement of the entire walk. In this sense, there is only 'one characteristic length'. When such a characteristic length is referred to, generically, it is customary to use the symbol ξ.

5.4 Functional Equations and Scaling: One Variable

We have seen that several different definitions of the characteristic length ξ all scale as $\sqrt{t}$. Equivalently, if $t(\xi)$ is the characteristic time for the ant to 'trace out' a domain of linear dimension ξ, then

$$t \sim \xi^2. \tag{5.18}$$

More formally, for all positive values of the parameter λ such that the product $\lambda\xi$ is large, $t(\xi)$ is, asymptotically, a *homogeneous function*,

$$t(\lambda^{1/2}\xi) = \lambda t(\xi). \tag{5.19}$$

Equation (5.19) is called a functional equation since it provides a constraint on the form of the function $t(\xi)$. In contrast, algebraic equations provide constraints on the numerical values of the quantities appearing in them. In fact, (5.18) is the 'solution' of the functional equation (5.19) in the sense that any function $t(\xi)$ satisfying (5.19) also satisfies (5.18) – we say that power laws are the solution to the functional equation (5.19). To see this, we note that if (5.19) holds for all values of the parameter λ, then it holds in particular when $\lambda = 1/\xi$. With this substitution, (5.19) reduces to (5.18).

It is also straightforward to verify that any function $t(\xi)$ obeying (5.18) obeys (5.19). Thus (5.19) implies (5.18) *and conversely*. This connection between power law behavior and a symmetry operation, called *scaling symmetry*, is at the root of the wide range of applicability of fractal concepts in physics.

5.5 Fractal Dimension of the Unbiased Random Walk

Writing (5.18) in the form

$$t \sim \xi^{d_f} \tag{5.20a}$$

exhibits the feature that the scaling exponent d_f explicitly reflects the asymptotic dependence of a characteristic 'volume' (the number of points in the trail of the ant) on a characteristic 'length' (R_g, R_{EE}, or $\mathcal{L}_k$). Thus for the random walk,

$d_f = 2$, but in general d_f is a kind of dimension. We call d_f the *fractal dimension* of the random walk.

If we write (5.19) in the form

$$t(\lambda\xi) = \lambda^{d_f} t(\xi), \tag{5.20b}$$

then we see that d_f plays the role of a scaling exponent governing the *rate* at which we must scale the time if we wish to trace out a walk of greater spatial extent. For example, if we wish a walk whose trail has twice the size, we must wait a time 2^{d_f}. Similarly, if we wish to 'design' a polymer with twice the radius of gyration, we must increase the molecular weight by the factor 2^{d_f}.

It is significant that the fractal dimension d_f of a random walk is 2, *regardless of the dimension of space*. This means that a time exposure of a 'drunken firefly' in three-dimensional space is an object with a well-defined dimension,

$$d_f = 2. \tag{5.21}$$

Similarly, a time exposure in a Euclidean space of any dimension d produces an object with the identical value of the fractal dimension, $d_f = 2$.

5.6 Universality Classes and Active Parameters

5.6.1 Biased Random Walk

Next we generalize to the case in which the motion of the ant is still random, but displays a bias favoring one direction over the other. We shall see that the bias has the effect of changing, *discontinuously*, the exponent characterizing the dependence on time of the characteristic length.

Let us place our ant again on a one-dimensional lattice, but now imagine that its coin is *biased*. The probability to be heads is

$$p \equiv \frac{1+\varepsilon}{2}, \tag{5.22}$$

while the probability to be tails is $q \equiv 1 - p = (1 - \varepsilon)/2$. From (5.22) we see that the parameter

$$\varepsilon = 2p - 1 = p - q. \tag{5.23}$$

defined in (5.22) is the difference in probabilities of heads and tails; ε is called the *bias*. We say that such an ant executes a *biased random walk*.

Although the results of the previous section will be recovered only in the case $\varepsilon = 0$, the same general concepts apply. The possible configurations of the biased walk are the same as for the unbiased random walk – i.e., we say that the phase space is the same. The values A_c associated with each configuration (each point in phase space) are also the same. However, instead of being identically $(1/2)^t$ for all configurations, the values of P_c now depend upon the configuration. If

events are uncorrelated, then the joint probability is simply the product of the separate probabilities. Hence

$$P_c = p^{h_c}(1-p)^{t-h_c}, \tag{5.24}$$

where h_c is the number of 'heads' in configuration c.

5.6.2 Scaling of the Characteristic Length

Now the expectation value $\langle x \rangle_t$ is not zero, as it was for the unbiased ant. Rather, we find that (5.8) is replaced by

$$\langle x \rangle_t = (p-q)t = \varepsilon t. \tag{5.25}$$

Thus the bias ε plays the role of the *drift velocity* of the center of mass of the probability cloud of the ant, since the time derivative of $\langle x \rangle_t$ is the analog of a velocity.

Other expectation values are also affected. For example, (5.9) generalizes to

$$\langle x^2 \rangle_t = [(p-q)t]^2 + 4pqt = \varepsilon^2 t^2 + (1-\varepsilon^2)t. \tag{5.26}$$

If $\varepsilon \equiv p - q = 0$, the results (5.25) and (5.26) reduce to (5.8) and (5.9). We thus recover the unbiased ant, for which the characteristic length ξ scales as $\sqrt{t}$. For any non-zero value of ε, no matter how small, we see from (5.25) and (5.26) that asymptotically

$$\mathcal{L}_k \equiv \sqrt[k]{\langle x^k \rangle} \sim t. \tag{5.27}$$

for $k = 1, 2$ respectively (the general-k result is a bit of an exercise!). Thus we conclude that the ξ scales linearly in time: the fractal dimension of the walk changes *discontinuously* with ε from $d_f = 1$ for all non-zero ε to $d_f = 2$ for $\varepsilon = 0$ (Fig. 5.3).

Systems with the same exponent are said to belong to the same *universality class*. We say that the biased walk belongs to the $d_f = 1$ universality class for all non-zero values of the parameter ε, and that it belongs to the $d_f = 2$ universality class for $\varepsilon = 0$. The term *active parameter* is used to describe a parameter such as ε which changes the universality class of a system.

Here is a paradox! The dependence of d_f on bias ε is a *discontinuous* function of ε, yet the actual motion of the ant cannot differ much as ε changes infinitesimally. To resolve this paradox, consider a specific example of a biased walk with an extremely small value of bias, say $\varepsilon_o = 10^{-6}$. The r.h.s. of (5.26) has two terms. If only the first term were present, the ant would simply 'drift' to the right with uniform velocity ε. If only the second term were present, the motion of the biased ant would be the same as that of the unbiased ant, except that the width of the probability distribution would be reduced by a factor $(1-\varepsilon^2)$. To see which term dominates, we express the r.h.s. as $[\varepsilon^2 t + 1]t$. We can now define

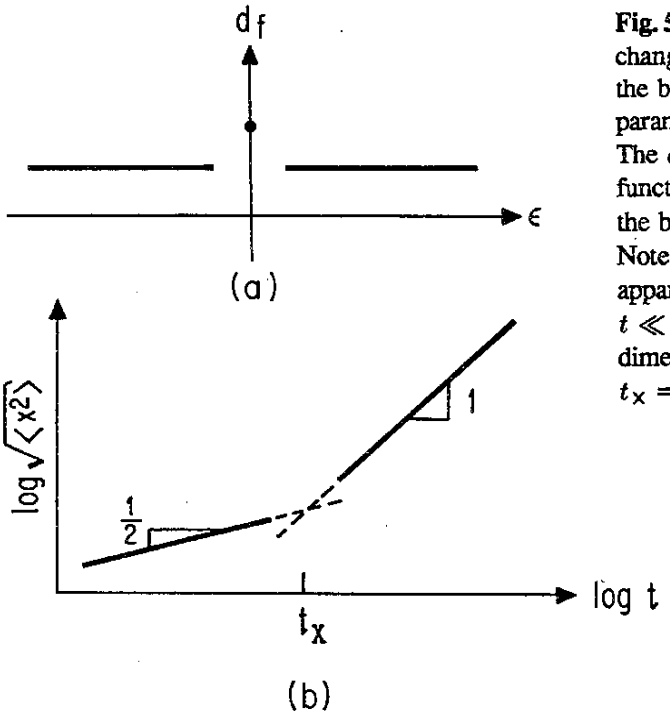

Fig. 5.3. (a) The *discontinuous* change in fractal dimension d_f for the biased random walk as the active parameter $\varepsilon \equiv p - q$ is varied. (b) The *continuous* change in $\langle x^2 \rangle$ as a function of time for a small value of the bias parameter $\varepsilon = p - q = 10^{-3}$. Note the crossover between the apparent fractal dimension $d_f = 2$ for $t \ll t_\times$ to the asymptotic fractal dimension $d_f = 1$ for $t \gg t_\times$, where $t_\times = 1/\varepsilon^2$ is the crossover time.

an important concept, the *crossover time* $t_\times = 1/\varepsilon^2$. For $t \ll t_\times$ the second term dominates and the ant has the statistics of an *unbiased* random walk; we say that the trail has an *apparent* fractal dimension $d_f = 2$. For $t \gg t_\times$, the first term dominates and the ant has the statistics of a *biased* random walk; the trail assumes its *true* or asymptotic fractal dimension $d_f = 1$ (Fig. 5.3b). Note that the crossover time $t_\times$ is quite large if the bias is small. If the bias is, say, 0.001, then the ant must walk a million steps before its trail becomes distinguishable from that of an unbiased ant!

Analogous considerations govern the crossover from one universality class to another in thermal critical phenomena, of the sort discussed in Chap. 4. Thus, e.g., if we have a three-dimensional magnet with interactions much weaker in the z direction, then far from the critical point the system displays apparent two-dimensional behavior, while close to the critical point it crosses over to its true asymptotic three-dimensional behavior. Thus we see that the important concepts of universality classes and the phenomenon of crossover between universality classes both have a geometric counterpart in the behavior of the biased random walk in the limit of small bias fields.

5.7 Functional Equations and Scaling: Two Variables

In this section we generalize the concept of a homogeneous function from one to two independent variables. We say a function $f(u, v)$ is a *generalized homogeneous function* if there exist two numbers a and b (termed scaling powers) such that for all positive values of the parameter λ, $f(u, v)$ obeys the obvious

generalization of (5.19),

$$f(\lambda^a u, \lambda^b v) = \lambda f(u, v). \tag{5.28}$$

We can see by inspection of (4.46c) that the free energy near the critical point obeys a functional equation of the form of (5.28), so generalized homogeneous functions must be important! To get a geometric feeling for such functions and their properties, consider the simple Bernoulli probability $\Pi(x,t)$ – the conditional probability that an ant is found at position x at time t given that the ant started at $x = 0$ at $t = 0$. In the *asymptotic* limit of large t, $\Pi(x,t)$ is expressible in closed form (unlike the free energy near the critical point!). The result is the familiar Gaussian probability density

$$\Pi_G(x,t) \equiv \frac{1}{\sqrt{2\pi t}} \exp\left[-\frac{x^2}{2t}\right], \tag{5.29}$$

Note that $\Pi_G(x,t)$ clearly satisfies (5.28), with scaling powers $a = -1$ and $b = -2$,

$$\Pi_G(\lambda^{-1}x, \lambda^{-2}t) = \lambda \Pi_G(x,t). \tag{5.30}$$

The predictions of the scaling relations (5.30) are given by the properties of generalized homogeneous functions. Among the most profound and useful of these properties is that of *data collapsing*. If (5.30) holds for all positive λ, then it must hold for the particular choice $\lambda = t^{1/2}$. With this choice, (5.30) becomes

$$\frac{\Pi_G(x,t)}{t^{-1/2}} = \Pi_G\left(\frac{x}{t^{1/2}}, 1\right) = \mathcal{F}(\tilde{x}), \tag{5.31a}$$

where we have defined the *scaled variable* $\tilde{x}$ by

$$\tilde{x} \equiv \frac{x}{t^{1/2}}. \tag{5.31b}$$

Equation (5.31a) states that if we 'scale' the probability distribution by dividing it by a power of t, then it becomes a function of a *single* scaled distance variable obtained by dividing x by a different power of t. Instead of data for $\Pi(x,t)$ falling on a family of curves, one for each value of t, data *collapse* onto a single curve given by the *scaling function* $\mathcal{F}(\tilde{x})$ (Fig. 5.4). This reduction from

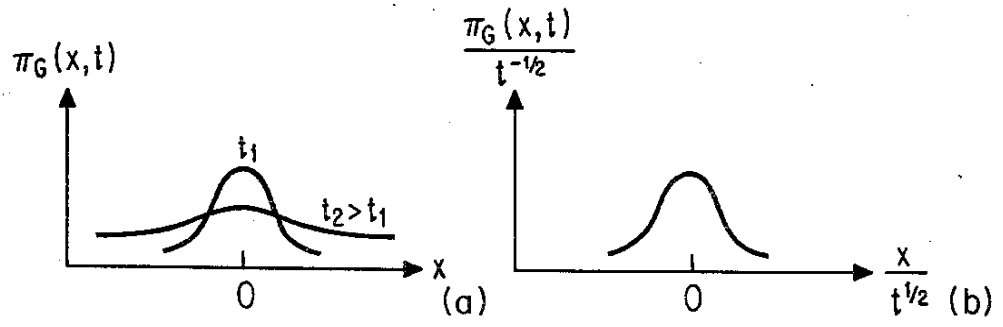

Fig. 5.4. Schematic illustration of scaling and data collapse as predicted by (5.31) for $\Pi_G(x,t)$, the Gaussian probability density.

a function of n variables to a function of $n-1$ *scaled* variables is a hallmark of fractals and scaling. The 'surprise' is that the function $\mathcal{F}(\tilde{x})$ defined in (5.31a) at first sight would seem to be a function of *two* variables, but it is in fact a function of only a single scaled variable $\tilde{x}$.

5.8 Fractals and the Critical Dimension

Thus far we have seen that the study of fractals help us in understanding two developments of modern theoretical physics:

- The empirical fact that the equation of state simplifies greatly in the vicinity of a critical point, and
- The empirical fact that diverse systems behave in the identical fashion near their respective critical points – a fact given the rather pretentious name *universality*.

Here we discuss one more simplification that occurs near critical points: above a certain *critical dimension* the mean field theory of Sect. 4.3.9 suffices to determine the critical exponents! This remarkable fact can be understood better using simple geometric concepts.

In Sect. 5.5.3, we introduced a geometric object with the same fractal properties as the trail of a random walk. This object is called a linear polymer, treated in the 'free-flight' approximation in which we can neglect the intersections of the chain with itself. Of course, no two objects can really occupy the same point in space, a fact known at least since the time of Archimedes' famous bathtub experiments. Hence the random walk model of a polymer chain cannot suffice to describe a real polymer. Instead, real polymers are modeled by a *self-avoiding walk* (SAW) in which a random walker must obey the 'global' constraint that he cannot intersect his own trail (Fig. 5.5).

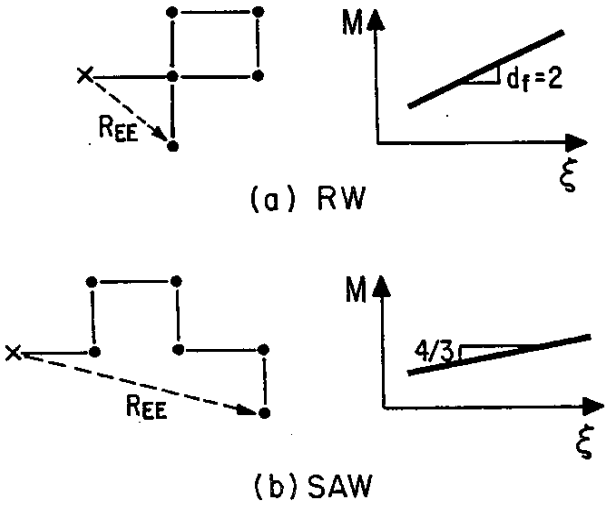

Fig. 5.5a–b. Schematic illustration of (a) a random walk, and (b) a self-avoiding walk (SAW). Each has taken 6 steps. We show just one of the 4^6 possible 6-step walks – many of these have zero weight for the SAW case. Shown also are schematic log-log plots showing how many steps are needed (the 'mass' M of the trail) for the walk to explore a region of characteristic size ξ, where here ξ is identified with the mean end-to-end distance R_{EE}.

A remarkable fact is that in sufficiently high spatial dimensions the SAW has the *identical* fractal dimension as the unbiased random walk, because in sufficiently high dimension the probability of intersection is so low as to be negligible. To see this, we first note that the *co-dimension* $d - d_f$ of the fractal trail is an exponent governing how the fraction of space 'carved out' by the trail decreases with length scale L, since from (5.1) ϱ decreases as $\varrho(L) \sim M(L)/L^d \sim (1/L)^{d-d_f}$. Now if two fractal sets with dimensions d_f' and d_f'' intersect in a set of dimension $d_\cap$, then the *sum* of the co-dimensions of the two sets is equal to the co-dimension of the intersection set,

$$d - d_\cap = (d - d_f') + (d - d_f''). \tag{5.32}$$

This general result follows from the fact that a site belongs to the intersection only if it belongs to both fractals: since statistically independent probabilities multiply (p. 116), the fraction of space (with exponent $d - d_\cap$) carved out by *both* fractals is the product of the fractions of space (with exponents $d - d_f'$ and $d - d_f''$) carved out by each.

To apply (5.32) to the trail of a random walk, consider the trail as being two semi-infinite trails – say red and blue – each with random walk statistics. If we substitute $d_f' = d_f'' = 2$ in (5.32), we find that for d equal to a critical dimension $d_c = 4$ the red and blue chains will intersect in a set of zero dimension. Thus for $d > d_c$, the 'classical' random walk suffices to describe the statistical properties of self-avoiding polymers!

The counterpart of this geometric statement is that the simple 'classical' theories presented in Chap. 4 give correct exponents for all dimensions above some critical dimension d_c. Indeed, this is one of the key results of recent years in theoretical physics. In this regard, we now introduce two generalizations of the simple Ising model which appear to be sufficient for describing almost all the universality classes necessary for understanding critical phenomena (Fig 5.6).

The first generalization of the Ising model is the Q-state Potts model. Each spin ζ_i localized on site i assumes one of Q *discrete orientations* $\zeta_i = 1, 2, \ldots, Q$. If two neighboring spins ζ_i and ζ_j have the same orientation, then they contribute an amount $-J$ to the energy, while if ζ_i and ζ_j are in different orientations, they contribute nothing. Thus the total energy of an entire configuration is

$$\mathcal{E}(Q) = -J \sum_{\langle ij \rangle} \delta(\zeta_i, \zeta_j), \tag{5.33a}$$

where

$$\delta(\zeta_i, \zeta_j) = \begin{cases} 1 & \text{if } \zeta_i = \zeta_j \\ 0 & \text{otherwise} \end{cases} \tag{5.33b}$$

The angular brackets in (5.33a) indicate that the summation is over all pairs of nearest-neighbor sites $\langle ij \rangle$. The interaction energy of a pair of neighboring parallel spins is $-J$, so that if $J > 0$, the system should order ferromagnetically at $T = 0$.

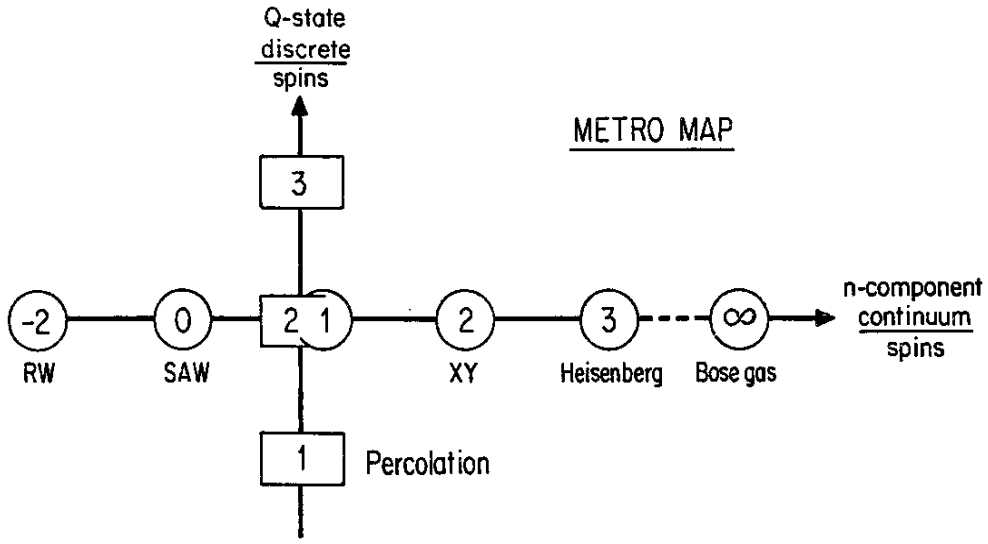

Fig. 5.6. Schematic illustration of a 'Metro map' showing how the Ising model has been generalized, first to form a 'North-South' line (allowing the two Ising spin orientations to become Q discrete orientations – the Potts model), and then to form an 'East-West' line (allowing the two spin orientations of the Ising model to be replaced by a continuum of spin orientations in an n-dimensional spin space – the n-vector model). The $n = 0$ station on the East-West Metro line corresponds to the self-avoiding random walk (SAW). Two additional stations on this line have the appealing feature that they correspond to models that are exactly soluble even for three spatial dimensions ($d = 3$): $n = -2$ (random walk model) and $n = \infty$ (the spherical model). The $Q = 1$ 'station' on the North-South Metro line corresponds to percolation and the $Q = 3$ station to a set of adsorption problems such as krypton on graphite.

The second generalization of the Ising model is the n-vector model. Each spin variable

$$\boldsymbol{S}_i \equiv (S_{i1}, S_{i2}, \ldots, S_{in}) \tag{5.34a}$$

is an n-dimensional unit vector

$$\sum_{\alpha=1}^{n} S_{i\alpha}^2 = 1, \tag{5.34b}$$

capable of taking on a *continuum of orientations*. Spin $\boldsymbol{S}_i$ localized on site i interacts isotropically with spin $\boldsymbol{S}_j$ localized on site j, so two neighboring spins contribute an amount $-J\boldsymbol{S}_i \cdot \boldsymbol{S}_j$ to the energy. Thus the total energy of a spin configuration is

$$\mathcal{E}(n) = -J \sum_{\langle ij \rangle} \boldsymbol{S}_i \cdot \boldsymbol{S}_j \tag{5.34c}$$

The key parameter in the Potts model is Q (the number of different discrete orientations of the spin variables), just as the key parameter in the n-vector model is n (the dimension of the spin $\boldsymbol{S}_i$). Together the Potts and n-vector models are sufficient to describe the behavior of a wide variety of systems near their critical

points, and as a result immense attention has been focussed on understanding these models.

For dimensions above a critical dimension d_c, the classical 'mean field' theory of Sect. 4.3.9 provides an adequate description of critical-point exponents and scaling functions, whereas for $d < d_c$, the classical theory breaks down in the immediate vicinity of the critical point because statistical fluctuations neglected in the classical theory become important. The case $d = d_c$ must be treated with great care; usually, the classical theory 'almost' holds, and the modifications take the form of weakly singular corrections.

For the n-vector model $d_c = 4$. Different values of d_c are usually found for multicritical points, such as occur when lines of critical points intersect. For example, $d_c = 3$ for a point where three critical lines intersect, and $d_c = 8/3$ for a fourth-order critical point. For a uniaxial ferromagnet or ferroelectric formed of interacting classical dipoles, $d_c = 3$; $LiTbF_4$ is one realization. In fact, $d_c = 2$ for certain structural phase transitions, such as that occurring in $PrAlO_3$.

In the models we have been considering, linear polymers can be thought of as linear clusters on a lattice. Similarly, branched polymers can be thought of as branched clusters. Such clusters are often called *lattice animals*, because they represent all the possible shapes that can be formed out of the constituent elements. Thus linear lattice animals that do not self-intersect (i.e., are loopless) are just the SAWs we discussed above. However, in general, lattice animals may branch and may form loops. Equation (5.32) may also be applied to lattice animals. The fractal dimension of a *random* branched object (without any restrictions) is $d_f = 4$. Hence we expect $d_c = 8$ for branched polymers, using an argument analogous to the argument for linear polymers that leads from (5.32) to the result $d_c = 4$ (Table 5.1).

Table 5.1. Comparison of some of the scaling properties of (a) self-avoiding walks (which model linear polymers), (b) lattice animals (which model branched polymers), and (c) percolation (which models gelation). The first line gives d_c, the critical dimension. The second line gives d_f, the fractal dimension, for $d \geq d_c$. The third line gives d_f^{RG}, the prediction of renormalization group expansions, for $d \leq d_c$ to first order in the parameter $\varepsilon = d_c - d$. The fourth and fifth lines give the results for dimensions three and two respectively.

	(a) SAW	(b) LATTICE ANIMAL	(c) PERCOLATION
d_c	4	8	6
$d_f(d \geq d_c)$	2	4	4
$d_f^{RG}(d \leq d_c)$	$2\left(1 - \frac{1}{8}\varepsilon\right)$	$4\left(1 - \frac{1}{9}\varepsilon\right)$	$4\left(1 - \frac{5}{42}\varepsilon\right)$
$d_f(d = 3)$	≈ 1.7	2 (exact)	≈ 2.5
$d_f(d = 2)$	4/3 (exact)	≈ 1.6	91/48 (exact)

A remarkable fact is that certain limiting cases of the Potts and n-vector models have a direct relation to geometrical objects that are fractal, and so these limits provide an intriguing connection between 'Physics & Geometry'. *Percolation*, e.g., is a simple geometrical model in which we study clusters formed when a fraction p of the bonds of a lattice are occupied randomly. As shown in Fig. 5.7, above a threshold value p_c a subset of these bonds form a macroscopic connected object called the *infinite cluster*, and the properties of the percolation model in the vicinity of p_c are not unlike the properties of a system of cross-linking polymers in the vicinity of the gelation transition. The statistical properties of percolation can be recovered from the Q-state Potts model if we carefully form the limit $Q \to 1$. In this correspondence, the variable $p - p_c$ in percolation corresponds to the variable $T - T_c$ in the magnetic system.

Similarly, if we carefully form the $n \to 0$ limit of the n-vector model, then we recover the statistical properties of the SAW. In this correspondence, it turns out that the inverse mass M^{-1} in the polymer system corresponds to $T - T_c$ in the magnetic system. Thus the limit of large molecular weight corresponds to a critical point; we say that a growing polymer chain exhibits the phenomenon of

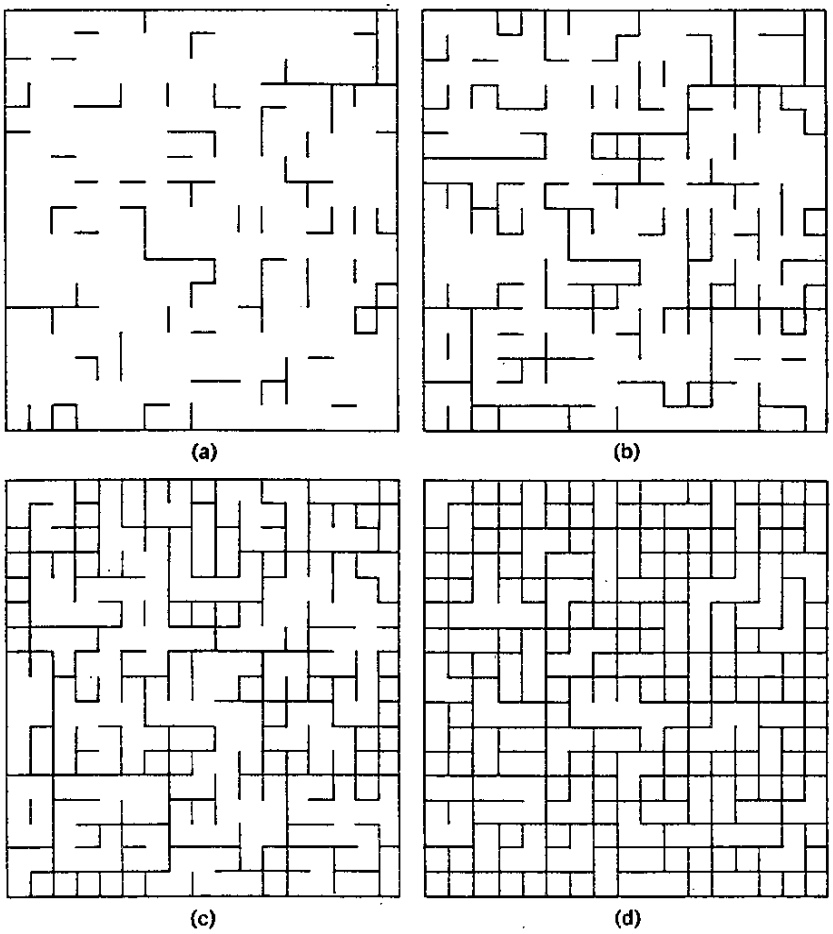

Fig. 5.7a–d. The phenomenon of bond percolation: a finite section of an infinite 'fence', in which a fraction p of the links is conducting while the remaining fraction $1 - p$ is insulating. Four choices of the parameter p are shown, (**a**), $p = 0.2$; (**b**), $p = 0.4$; (**c**), $p = 0.6$; and (**d**), $p = 0.8$.

self-organized criticality because as it grows it approaches a critical point. As a result, we expect quantities such as the polymer diameter to be characterized by universal behavior. In addition, the existence of a phase transition allows us to apply to the SAW problem modern techniques as the renormalization group. The use of fractal geometry (which concerns the limit $M \to \infty$) becomes relevant to studying materials near their critical points (which concern the asymptotic limit $T \to T_c$).

Theoretical physicists – for all their well-honed mathematical skills – are totally incapable of solving simply-defined models such as the Ising model or the SAW problem for the case of a three-dimensional ($d = 3$) system. However they can invent bizarre spin dimensionalities which do yield to exact solution in $d = 3$ and so provide useful 'anchor points' with which to compare the results of various approximation procedures. For example, for $n = -2$ the n-vector model is found to provide the same statistical properties as for the simple unbiased random walk (the limiting case of a *non-interacting* polymer chain). In the limit $n \to \infty$ we recover a model – termed the spherical model – which has the important features of being exactly soluble for all spatial dimensions d, as well as being useful in describing the statistical properties of the Bose-Einstein condensation.

5.9 Fractal Aggregates

We began our dessert by forming a simple non-random fractal aggregate, the Sierpinski gasket. We shall end the dessert by describing one of the most popular current models for random fractal aggregates, diffusion limited aggregation (DLA).

Like many models in statistical mechanics, the rule defining DLA is simple. At time 1, we place in the center of a computer screen a white pixel, and release a random walker from a large circle surrounding the white pixel. The four perimeter

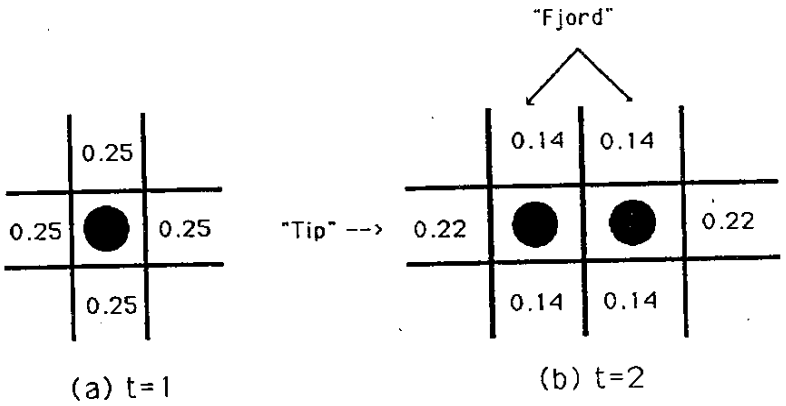

Fig. 5.8. (a) Square lattice DLA at time $t = 1$, showing the four growth sites, each with growth probability $p_i = 1/4$. (b) DLA at time $t = 2$, with 6 growth sites, and their corresponding growth probabilities p_i.

sites have an equal *a priori* probability p_i to be stepped on by the random walker (Fig. 5.8a), so we write

$$p_i = \tfrac{1}{4} \qquad (i = 1, \ldots, 4). \tag{5.35a}$$

The rule is that the random walker remains fixed at a perimeter site if and when it ever lands on the perimeter site – thereby forming a cluster of mass $M = 2$. There are $N_p = 6$ possible sites, henceforth called *growth sites* (Fig. 5.8b), but now the probabilities are *not* all identical: each of the growth sites of the two tips has growth probability $p_{\max} \cong 0.22$, while each of the four growth sites on the sides has growth probability $p_{\min} \cong 0.14$. Since a site on the tip is 50% more likely to grow than a site on the sides, the next site is more likely to be added to the tip – it is like capitalism in that 'the rich get richer.' One of the main features of recent approaches to DLA is that instead of focusing on the tips who are 'getting richer', we can focus on the fjords who are 'getting poorer' – which is a realization in Nature of the familiar experience that 'once you get behind you stay behind!'

Just because the third particle is *more likely* to stick at the tip does not mean that the next particle *will* stick on the tip. Indeed, the most that we can say about the cluster is to specify the *growth site probability distribution* – i.e., the set of numbers,

$$\{p_i\} \qquad i = 1, \ldots, N_p, \tag{5.35b}$$

where p_i is the probability that perimeter site ("growth site") i is the next to grow, and N_p is the total number of perimeter sites ($N_p = 4, 6$ for the cases $M = 1, 2$ shown in Figs. 5.5a and 5.5b respectively). The recognition that the set of $\{p_i\}$ gives us essentially the *maximum* amount of information we can have about the system is connected to the fact that tremendous attention has been paid to these p_i – and to the analogs of the p_i in various closely-related systems.

If the DLA growth rule is simply iterated, then we obtain a large cluster characterized by a range of growth probabilities that spans several orders of magnitude – from the tips to the fjords. The cover shows such a large cluster, where each pixel is colored according to the time it was added to the aggregate. From the fact that the 'last to arrive' particles (green pixels) are never found to be adjacent to the 'first to arrive" particles (white pixels), we conclude that the p_i for the growth sites on the tips must be vastly larger than the p_i for the growth sites in the fjords.

Until relatively recently, most of the theoretical attention paid to DLA has focussed on its fractal dimension. Although we now have estimates of d_f that are accurate to roughly 1%, we lack any way to *interpret* this estimate. This is in contrast to both the $d = 2$ Ising model and $d = 2$ percolation, where we can calculate the various exponents *and* interpret them in terms of 'scaling powers.' What we can interpret, however, is the distribution function $\mathcal{D}(p_i)$ which describes the histogram of the number of perimeter sites with growth probability p_i. The key idea is to focus on how this distribution function $\mathcal{D}(p_i)$ *changes* as the cluster mass M increases. The reason why this approach *is* fruitful is that

the $\{p_i\}$ contain the maximum information we can possibly extract about the dynamics of the growth of DLA. Indeed, specifying the $\{p_i\}$ is analogous to specifying the four 'growth' probabilities $p_i = 1/4$ $[i = 1, \cdots, 4]$ for a random walker on a square lattice.

The set of numbers $\{p_i\}$ may be used to construct a histogram $\mathcal{D}(\ln p_i)$. This distribution function can be described by its *moments*,

$$Z_\beta \equiv \sum_{\ln p} \mathcal{D}(\ln p)\, \mathrm{e}^{-\beta(-\ln p)}, \tag{5.36a}$$

which is a more complex way of writing

$$Z_\beta = \sum_i p_i^\beta. \tag{5.36b}$$

It is also customary to define a dimensionless 'free energy" $F(\beta)$ by the relation

$$F(\beta) = -\frac{\log Z_\beta}{\log L}. \tag{5.37a}$$

which can be written in the suggestive form

$$Z_\beta = L^{-F(\beta)}, \tag{5.37b}$$

The form (5.36a) as well as the notation used suggests that we think of β as an *inverse temperature*, $-\ln p/\ln L$ as an *energy*, and Z_β as a *partition function*. The notation we have used is suggestive of thermodynamics. Indeed, the function $F(\beta)$ has many of the properties of a free energy function – for example, it is a convex function of its argument and can even display a singularity or 'phase transition'. However for most critical phenomena problems, exponents describing moments of distribution functions are linear in their arguments, while for DLA $F(\beta)$ is not linear – we call such behavior *multifractal*. Multifractal behavior is characteristic of random multiplicative processes, such as arise when we multiply together a string of random numbers, and can be interpreted as partitioning a DLA cluster into fractal subsets, each with its own fractal dimension (Plate 1).

Our dessert is now finished, so let us take a little exercise to work off the calories. Our exercise takes the form of a simple *hands-on* demonstration that enables us to actually 'see with our eyes' (a) that DLA is a fractal and (b) that its fractal dimension is approximately 1.7. We begin with a large DLA cluster (Plate 1), and cut out from three sheets of scrap paper holes of sizes $L = 1, 10, 100$ (in units of the pixel size). Now cover the fractal with each sheet of paper, and estimate the fraction of the box that is occupied by the DLA. This fraction should scale in the same way as the density $\varrho(L) \equiv M(L)/L^2$ which, from (5.4), decreases with increasing length scale as $\varrho(L) = \mathcal{A} L^{d_f - 2}$. Now (5.4) is mathematically equivalent to the functional equation

$$\varrho(\lambda L) = \lambda^{d_f - d} \varrho(L). \tag{5.38a}$$

For our exercise, $\lambda = 10$ and we find

$$\varrho(L) \approx \begin{cases} 1 & L = 1 \\ 1/2 & L = 10 \\ 1/4 & L = 100 \end{cases} . \tag{5.38b}$$

Here the result of (5.38b),

$$\varrho(10L) \approx \tfrac{1}{2}\varrho(L), \tag{5.38c}$$

convinces us that $10^{d_f - 2} \approx \frac{1}{2}$, leading to $d_f - 2 \approx \log_{10} \frac{1}{2} = -0.301$, or

$$d_f \approx 1.70. \tag{5.39a}$$

This crude estimate agrees with the most accurate calculated value,

$$d_f = 1.715 \pm 0.004, \tag{5.39b}$$

based on clusters with 10^6 particles (P. Meakin, 1990 private communication).

5.10 Fractals in Nature

The reader has savored the meal, indulged himself on the dessert, and is now entitled to a little fantasy before falling asleep for the night. Accordingly, we shall describe in this final section some of the situations in Nature where fractal phenomena arise and wax philosophical about exactly how much theoretical physics might hope to contribute to our understanding of these phenomena.

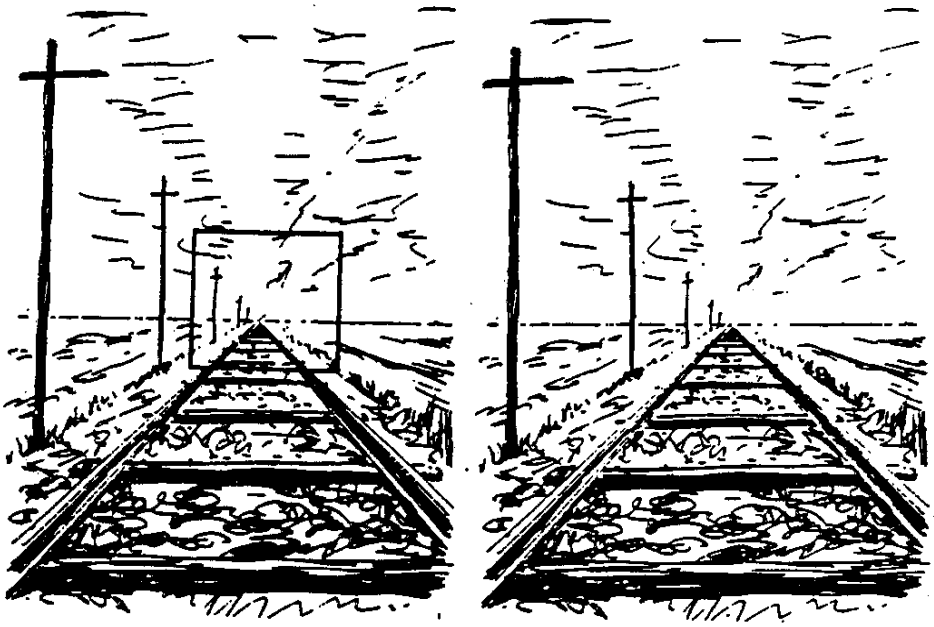

Fig. 5.9. Schematic illustrations of scale invariance for a blow-up of the central portion of a photograph from the rear of a train in a flat terrain like Oklahoma.

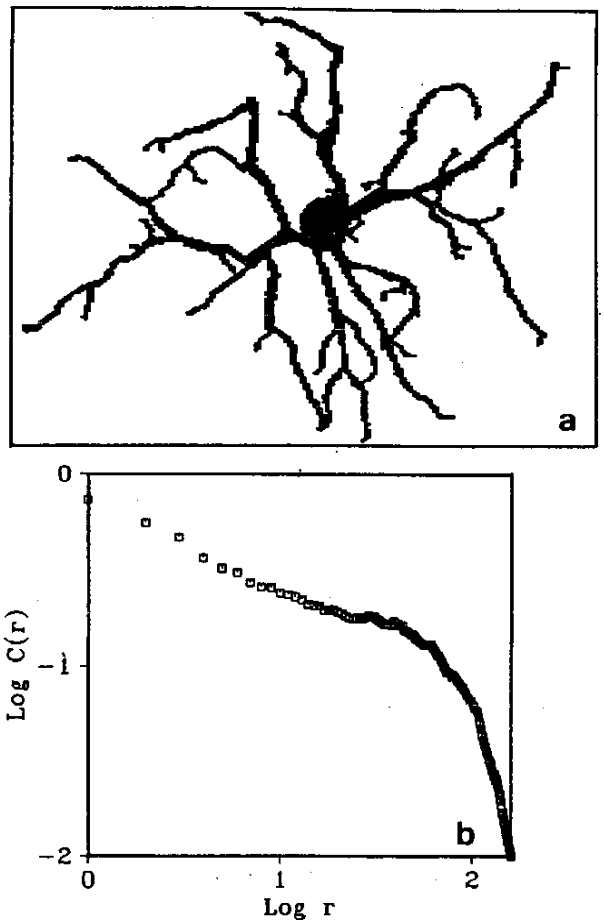

Fig. 5.10. Typical retinal neuron and its fractal analysis. The correlation function $C(r)$ in scales in the same fashion as the density, given by (5.4). (*See* F. Caserta, H.E. Stanley, W. Eldred, G. Daccord, R. Hausman, and J. Nittmann, "Physical Mechanisms Underlying Neurite Outgrowth: A Quantitative Analysis of Neuronal Shape", Phys. Rev. Lett. **64**, 95 (1990).)

Everyone has seen many fractal objects – probably at an early stage in life. Perhaps we once photographed scenery from the back of a train and noticed that the photograph looked the same at all stages of enlargement (Fig. 5.9). Perhaps we noticed that the Metro of Paris has a fractal structure in the suburbs (M. Benguigui and M. Daoud, 1990 preprint). Perhaps we saw that snow crystals all have the same pattern, each part of a branch being similar to itself. In fact, to 'see' something at all – fractal or non-fractal – requires that the nerve cells in the eye's retina must send a signal, and these retinal nerve cells are themselves fractal objects (Fig. 5.10).

There are many *caveats* that we must pay heed to. To be fractal implies that a part of the object resembles the whole object, just as the branches of a DLA look similar to the whole structure and also similar to the sub-branches. The Sierpinski gasket shows this self-similarity exactly, whereas for DLA and other random fractals this self-similarity is only statistical. Fractal objects in Nature are random fractals, so the self-similarity we discover by enlarging the middle section of Fig. 5.9 is replaced by a self-similarity obtained only by averaging together many realizations of the same object.

The second *caveat* is that fractals in Nature are not fractal on all length scales. There is a range of length scales, followed by an inevitable crossover to homogeneous behavior. We can indicate this fact using the Sierpinski gasket model of Sect. 5.1 by simply starting, after n stages, to aggregate exact copies of the object, so that asymptotically one obtains a homogeneous object made

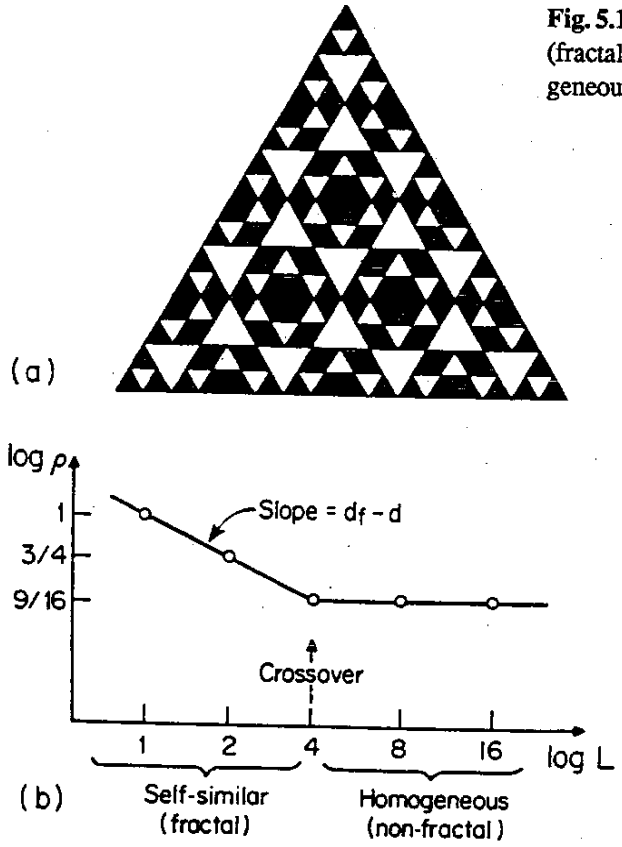

Fig. 5.11a,b. A Sierpinski gasket that is self-similar (fractal) on small length scales, but becomes homogeneous (non-fractal) on large length scales.

up of units each identical to the n-stage Sierpinski gasket (Fig. 5.11). The result is a crossover phenomenon. This example is instructive, because the resulting behavior is analogous to what is usually found in Nature: real objects do not remain fractal for all scales, but instead are fractal over typically a factor of 10 or 100 in length scale. The fact that real objects in Nature do not remain fractal on all length scales does not make them any less interesting – there can even be useful information in the value of the length scale on which the crossover to homogeneous behavior occurs.

With these caveats, however, it is a fact that fractals abound in Nature. In fact, almost any object for which randomness is the basic factor determining the structure will turn out to be fractal over some range of length scales – for much the same reason that the simple random walk is fractal: there is nothing in the microscopic rules that can set a length scale so the resulting macroscopic form is 'scale-free'...scale-free objects obey power laws and lead to functional equations of the form of (5.19) and (5.28).

Today, there are roughly of order 10^3 fractal systems in Nature, though a decade ago when Mandelbrot's classic was written, many of these systems were not known to be fractal. These include examples of relevance to a wide variety of fields, ranging from geological chemistry (Plate 3) and fracture mechanisms (Plate 4) on the one hand, to fluid turbulence (Plate 5) and the "molecule of life" – water (Plate 6) – on the other. DLA alone has about 50 realizations in physical systems. DLA models aggregation phenomena described by a Laplace equation ($\nabla^2 \Pi(r,t) = 0$) for the probability $\Pi(r,t)$ that a walker is at position r and time t. More surprising is the fact that DLA describes a vast range of phenomena that

at first sight seem to have nothing to do with random walkers. These include fluid-fluid displacement phenomena ("viscous fingers"), for which the pressure P at every point satisfies a Laplace equation (Plates 7–10). Similarly, dielectric breakdown phenomena, chemical dissolution (Plate 11), electrodeposition, and a host of other phenomena may be members of a suitably-defined *DLA universality class*. If anisotropy is added, then DLA describes dendritic crystal growth and snowflake growth (Fig. 5.12). The dynamics of DLA growth can be studied by the multifractal analysis discussed above, or by decomposing a DLA cluster into active tips connected to the central seed by a "skeleton" from which emanate a fractal hierarchy of branches whose dynamics resembles $1/f$ noise (Plate 12).

Recently, several phenomena of *biological* interest have attracted the attention of DLA *aficionados*. These include the growth of bacterial colonies, the retinal vasculature, and neuronal outgrowth (Fig. 5.10). The last example is particularly intriguing: if evolution indeed chose DLA as the morphology for the nerve cell, then can we understand 'why' this choice was made? What evolutionary advantage does a DLA morphology convey? Is it significant that the Paris Metro evolved with a similar morphology or is this fact just a coincidence? Can

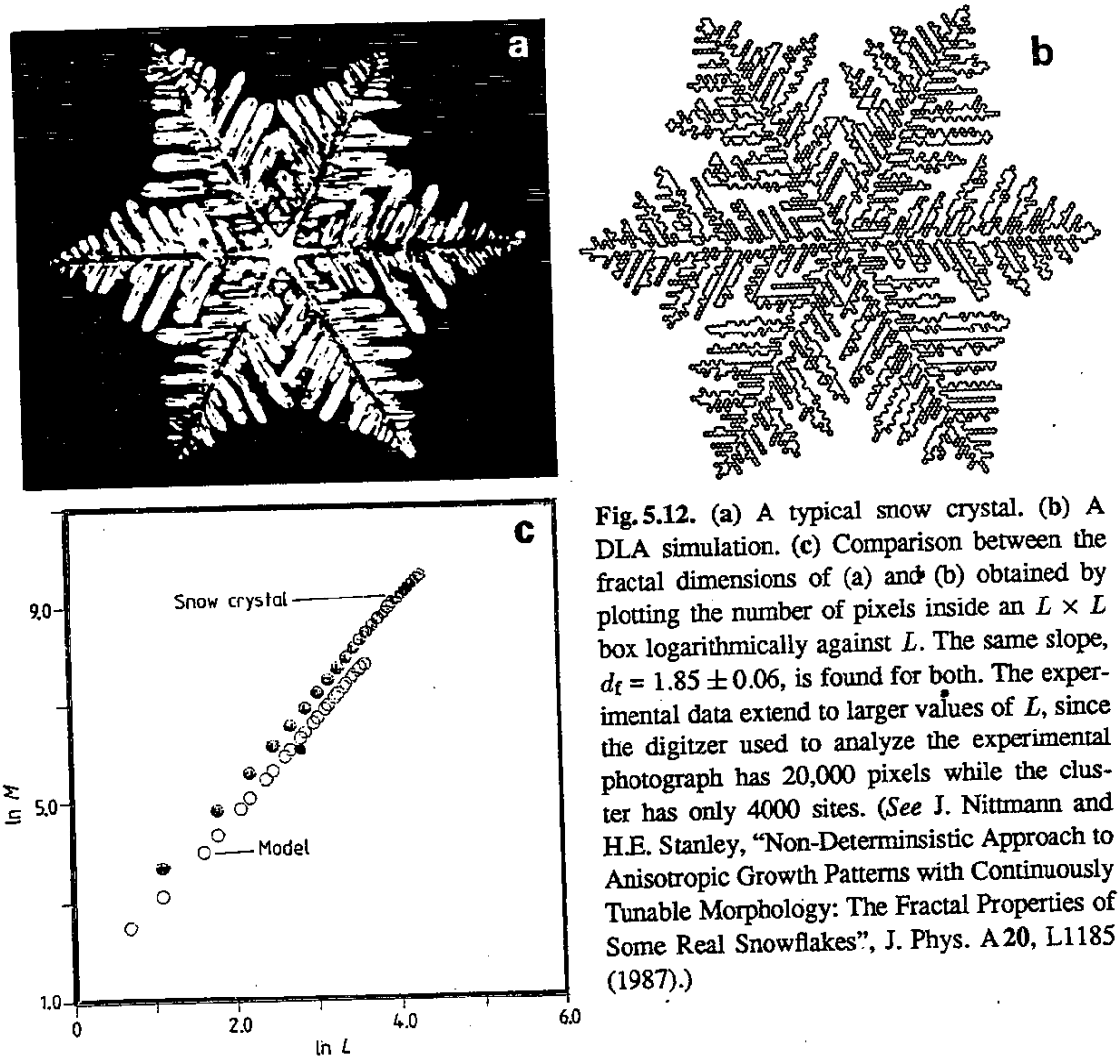

Fig. 5.12. (a) A typical snow crystal. (b) A DLA simulation. (c) Comparison between the fractal dimensions of (a) and (b) obtained by plotting the number of pixels inside an $L \times L$ box logarithmically against L. The same slope, $d_f = 1.85 \pm 0.06$, is found for both. The experimental data extend to larger values of L, since the digitzer used to analyze the experimental photograph has 20,000 pixels while the cluster has only 4000 sites. (*See* J. Nittmann and H.E. Stanley, "Non-Determinsistic Approach to Anisotropic Growth Patterns with Continuously Tunable Morphology: The Fractal Properties of Some Real Snowflakes", J. Phys. A **20**, L1185 (1987).)

we use the answer to these questions to better design the next generation of computers? These are important issues that we cannot hope to resolve quickly, but already we appreciate that a fractal object is the most efficient way to obtain a great deal of intercell 'connectivity' with a minimum of 'cell volume', so the key question is 'which' fractal did evolution select, and why?

It is awe-inspiring that remarkably complex objects in Nature can be quantitatively characterized by a single number, d_f. It is equally awe-inspiring that such complex objects can be described by various models with extremely simple rules. It is also an intriguing fact that even though no two natural fractal objects that we are likely to ever see are identical, nonetheless every DLA has a generic 'form' that even a child can recognize. The analogous statement holds for many random structures in Nature. For example no two snowflakes are the same yet every snowflake has a generic form that a child can recognize

Perhaps most remarkable to a student of theoretical physics is the fact that simple geometrical models – with no Boltzmann factors – suffice to capture features of real statistical mechanical systems such as those discussed in Chap. 4. What does this mean? If we understand the essential physics of an extremely robust model, such as the Ising model, then we say that we understand the essential physics of the complex materials that fall into the universality class described by the Ising model. In fact, by understanding the pure Ising model, we can even understand most of the features of *variants* of the Ising model (such as the n-vector model) that may be appropriate for describing even more complex materials. Similarly, we feel that if we can understand DLA, then we are well on our way to understanding *variants* of DLA, such as DLA with noise reduction (Plate 13), the screened growth model (Plate 14), ballistic deposition (Plate 15), and cluster–cluster aggregation (Plate 16).